Static analysis of an under-actuated bio-inspired robot

Nicolas J S Testard, Christine Chevallereau, Philippe Wenger

Static analysis of an under-actuated bio-inspired robot

Nicolas J.S. Testard, Christine Chevallereau, Philippe Wenger

January 12, 2024

1 Introduction

The human neck is comprised of seven vertebrae, offering a relatively limited range of motion. In contrast, bird necks possess a higher number of vertebrae, typically ranging between 11 and 25. This increased vertebral count provides birds with the ability to execute more intricate and dexterous movements, facilitated by a sophisticated network of tendons and muscles. Such neck dexterity enables birds to employ their necks analogously to how humans use their arms, allowing them to grasp and manipulate objects. Furthermore, birds' necks exhibit remarkable speed in motion, as exemplified by the rapid pecking movements of woodpeckers.

The exploration of bird neck performances has inspired the development of new robots. In a study by Furet et al. [1], the motion between bird neck vertebrae was investigated. It was observed that the motion between two vertebrae could involve either a pure rotation or a rolling motion of an ellipse on another. Pure rotation can be replicated using a revolute joint, while the rolling of ellipses can be modeled with an anti-parallelogram joint, also known as *X-joints* [2]. These joints, discussed in [3], can be actuated using two antagonistic cables to simulate the effects of muscles and tendons. Notably, research by Muralidharan et al. [4] highlights that revolute joints lack co-actuation properties compared to X-joints, making the latter more attractive for the development of bio-inspired robots.

In a study conducted by Fasquelle et al. [5], a fully-actuated robot comprising three X-joints and four cables was successfully built and controlled, demonstrating the feasibility of the mechanism. In the context of mechanisms inspired by the bird neck, where the aim is to limit the number of actuators, the use of a restricted number of cables becomes an interesting consideration. In such cases, the system under investigation becomes underactuated. The objective of this report is to examine the impact of cables in statics on underactuated robots constructed with X-joints actuated by antagonistic cables.

Section 2 provides an overview of the underactuated robots under study. In Section 3, the influence of cable tensions on the robot is explored, revealing that an increase in cable tensions leads the robot to converge to a predictable configuration, regardless of the mass and elastic parameters. The report concludes with Section 4.

2 Presentation of the robots

This report focuses on the analysis of two robots depicted in Fig. 1. The first robot consists of 2 X-joints actuated by 2 cables, each pulling on the left and right sides of the joints. The second robot comprises 6 X-joints and is actuated by 4 cables. One cable pulls all joints on one side, while the remaining three cables pull two joints each on the other side. This cable routing is inspired by nature, resembling the structure found in certain bird species where a long ventral muscle pulls several vertebrae. Both robots are underactuated since two joints linked by the same cables cannot move independently from one another. Additionally, springs are incorporated in parallel with the cables to maintain a stable configuration at rest.

We will consider $b = 0.05$ m, $L = 0.1$ m, a mass of 0.16 kg for the top bar, and 0.026 kg for the diagonal bars.

Each joint i has one degree of freedom, which is defined as the orientation of the top bar compared to the base bar α_i. The static model has been computed in [6] [7] and is given by:

$$\boldsymbol{g}(\boldsymbol{\alpha}) = \mathbf{Z}(\boldsymbol{\alpha})\boldsymbol{f} \tag{1}$$

where:

- $\boldsymbol{\alpha}$ is the vector of the joint angles.
- $\boldsymbol{g}(\boldsymbol{\alpha})$ represents the effects of gravity and the springs.

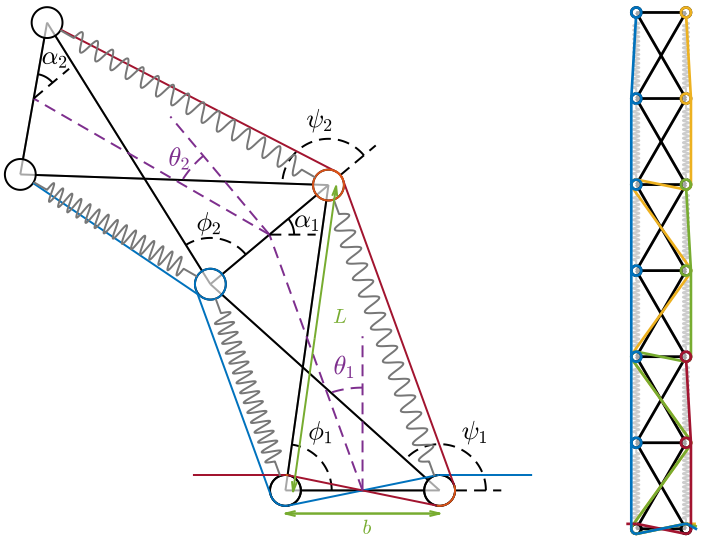

Figure 1: Representation of and under-actuated robots with 2 joints and 2 cables and another one with 6 joints and 4 cables

- $\mathbf{Z}(\boldsymbol{\alpha}) = -\dfrac{d\boldsymbol{l}}{d\boldsymbol{\alpha}}^{\top}$, with $\boldsymbol{l}$ as the vector of cable lengths.
- $\boldsymbol{f}$ is the vector of cable tensions.

3 Effect of the cable tensions

The objective of this section is to investigate the impact of minimal cable tensions on the overall equilibrium of the underactuated robots. The matrix $\mathbf{Z}$ has a rank of N_c, where N_c is the number of cables. However, during control, only $N_c - 1$ degrees of freedom are controllable, as one is designated to maintain the cable tensions positive.

For instance, in the case of the robot with 6 joints and 4 cables, only 3 degrees of freedom are controllable. These degrees of freedom can be represented by the end-effector position and orientation, denoted as $\boldsymbol{X} = [x, y, \gamma]^{\top} = \boldsymbol{f}_X(\boldsymbol{\alpha})$. Given a desired end effector position and orientation $\boldsymbol{X}_{des}$, the static equilibrium position of the robot can be calculated as follows:

$$\begin{aligned} (\boldsymbol{\alpha}, \boldsymbol{f}) = \min_{\boldsymbol{\alpha}, \boldsymbol{f}} \; & ||\boldsymbol{f}|| \\ & \boldsymbol{g}(\boldsymbol{\alpha}) = \mathbf{Z}(\boldsymbol{\alpha})\boldsymbol{f} \\ s.t. \; & \boldsymbol{f}_X(\boldsymbol{\alpha}) = \boldsymbol{X}_{des} \\ & min(\boldsymbol{f}) \geq f_{min} \end{aligned} \tag{2}$$

The springs are assumed to be symmetric on the right and left sides, with stiffness values from bottom to top of $[1000, 850, 800, 650, 400, 250]$ N/m. They have a free length of 0.046 m, an initial orientation of $\pi/4$, and are subject to gravity. Additionally, the pulley radius is considered to be null ($R_p = 0$).

Figure 2 illustrates the variation of $\boldsymbol{\alpha}$ for a given $\boldsymbol{X}_{des}$, accompanied by the corresponding cable tensions depicted in Figure 3, as the minimal cable tension f_{min} is modified. These figures indicate that as tensions increase, the robot converges to a configuration where joints actuated by the same cables have identical angles. Specifically, it converges to a position where the $\mathbf{Z}$ matrix loses one rank, as shown in Figure 4. Two different robot configurations for distinct minimal tensions are presented in Figure 5, demonstrating that $\boldsymbol{X}$ remains constant while joints angles $\boldsymbol{\alpha}$ differ.

In the presence of a non-null pulley radius ($R_p \neq 0$), Figure 6 demonstrates that the robot converges to a configuration where the angles linked by actuation have different values. However, in this configuration, the rank of the matrix $\mathbf{Z}$ decreases by 1, as illustrated in Figure 7.

The decrease in rank of $\mathbf{Z}$ can be explained. We express $\boldsymbol{f} = \boldsymbol{c} f_L$, where $\boldsymbol{c}$ is a vector of constants expressing the ratio between the cable tensions (compared to the left cable tension). The static equation can therefore be written as:

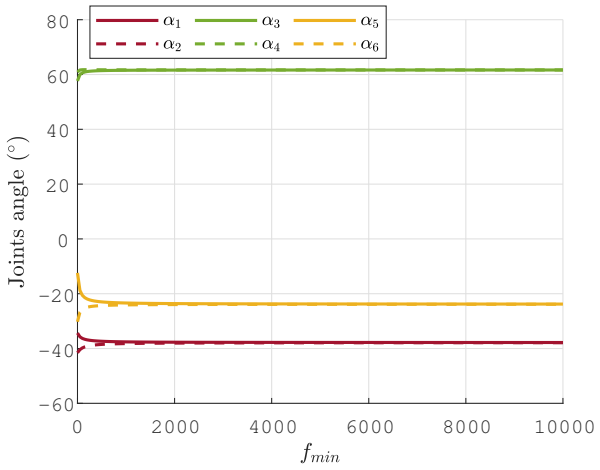

Figure 2: Evolution of the robot joint angle for a set $\boldsymbol{X}_{des}$ depending on the minimal tension (null pulley radius)

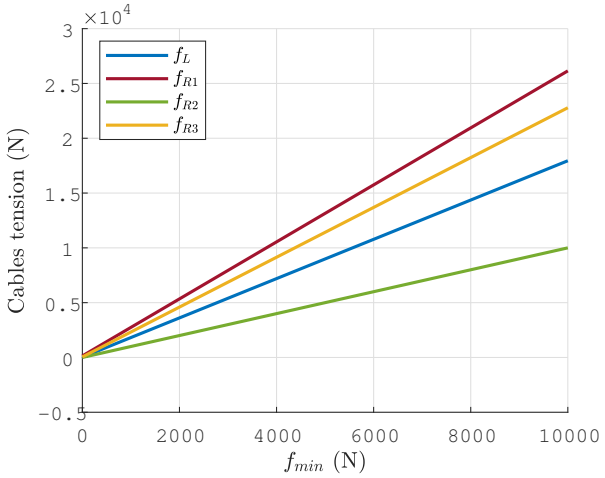

Figure 3: Evolution of the cable tensions for a given $\boldsymbol{X}$ when the minimal tension increase.

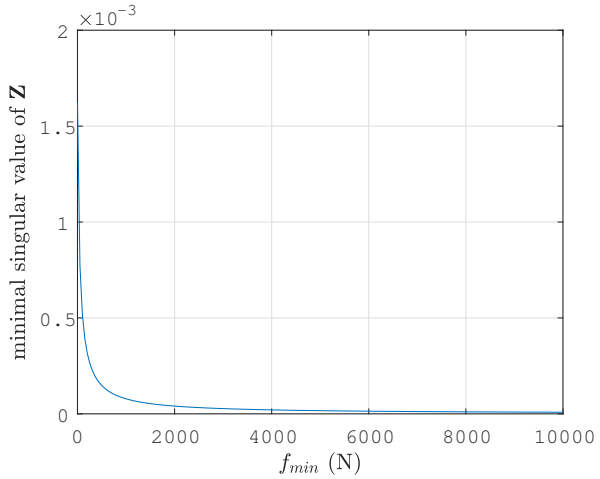

Figure 4: Evolution of the minimal singular value of $\mathbf{Z}$ for a set $\boldsymbol{X}_{des}$ depending on the minimal tension (null pulley radius)

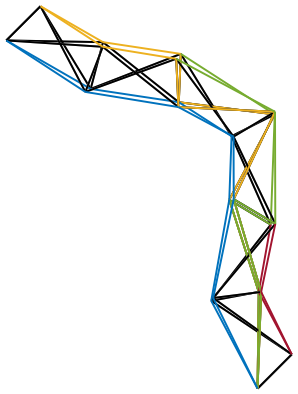

Figure 5: Position of the robot for a given $\boldsymbol{X}_{des}$ for a minimal tension of 0N and of 10000N. (springs are hidden for lisibility)

$$\mathbf{Z}(\boldsymbol{\alpha})\boldsymbol{c} = \frac{1}{f_L}\boldsymbol{g}(\boldsymbol{\alpha}) \tag{3}$$

Thus, it can be observed that as the cable tensions approach infinity ($f_L \to +\infty$), $\boldsymbol{c}$ becomes a null space vector of the $\mathbf{Z}$ matrix, and consequently, the rank of $\mathbf{Z}$ decreases.

For example, for the robot with 2 joints and 2 cables, we have $\boldsymbol{f} = [f_L, f_R]$, where f_L and f_R are the tensions in the left and right cables, respectively. Moreover, by defining $\boldsymbol{c} = [1, c]$ with $c = f_R/f_L$ and solving the $\mathbf{Z}(\boldsymbol{\alpha})\boldsymbol{c}$ for different values of c, it is possible to predict the position of the robot when the cable tensions increase, as presented in Fig. 8 and 9.

We set spring stiffnesses to 100 N/m and 600 N/m on the left of the first joint and 500 N/m and 200 N/m on the right of the first joint. In the presence of gravity and a null pulley radius, Fig. 10 and 11 show the evolution of the joint angles in simulation [8], when the cable tensions are increasing with a constant ratio. In Fig. 10, the ratio is $c = 1$, and the joint angles converge to 0° as expected by Fig. 8. Similarly, in Fig. 11, $c = 0.61676$, and the joint angles converge to 50° as expected by Fig. 8. Thus, these figures confirm the evolution of the joint angles to a configuration where the rank of $\mathbf{Z}$ decreases when the cable tensions go to infinity.

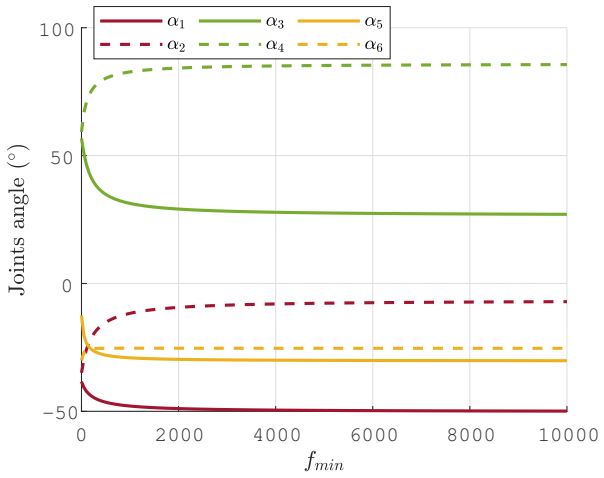

Figure 6: Evolution of the robot joint angle for a set $\boldsymbol{X}_{des}$ depending on the minimal tension (pulley radius of 0.01 m)

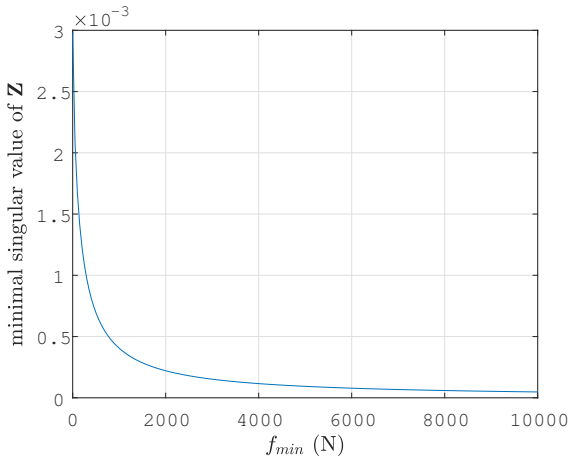

Figure 7: Evolution of the minimal singular value of $\mathbf{Z}$ for a set $\boldsymbol{X}_{des}$ depending on the minimal tension (pulley radius of 0.01 m)

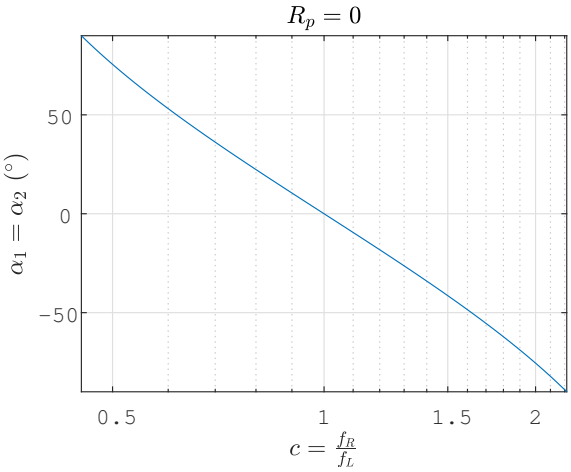

Figure 8: Evolution of the equal robot joint angle depending on the ratio between the cable tension when there is infinite tension (null pulley radius)

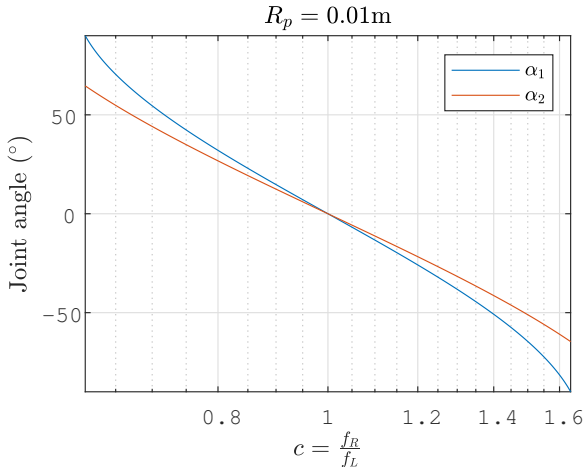

Figure 9: Evolution of the robot joint angle depending on the ratio between the cable tension when there is infinite tension (pulley radius of 0.01 m)

4 Conclusion

This report has presented under-actuated robots inspired by the bird neck. These robots are built with X-joints that are actuated through 2 antagonistic cables.

It has been shown that as cable tensions are increased, robots converge to a configuration where the rank of the actuation matrix $\mathbf{Z}$ decreases by one. This indicates that only $N_c - 1$ degrees of freedom can be freely controlled, while the remaining one, used for maintaining the positivity of the cable tensions, has less impact.

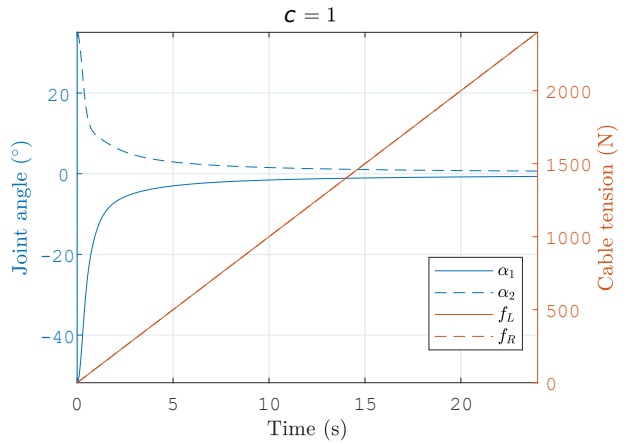

Figure 10: Simulation of the joint angle evolution when the tensions are increase with a ratio $c = 1$ with $R_p = 0$

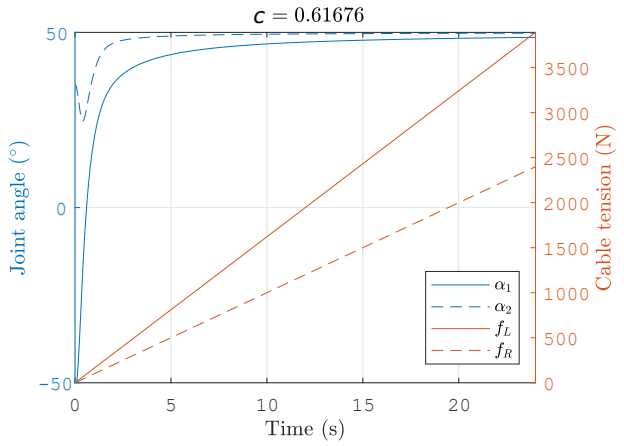

Figure 11: Simulation of the joint angle evolution when the tensions are increase with a ratio $c = 0.61676$ with $R_p = 0$

References

[1] M. Furet, A. Abourachid, C. Böhmer, V. Chummun, C. Chevallereau, R. Cornette, X. De La Bernardie, and P. Wenger, "Estimating motion between avian vertebrae by contact modeling of joint surfaces," Computer Methods in Biomechanics and Biomedical Engineering, vol. 25, pp. 123–131, Jan. 2022. Publisher: Taylor & Francis.

[2] K. D. Snelson, "Continuous tension, discontinuous compression structures," US Patent 3169611, Feb. 1965.

[3] H. Stachel, "Flexible Cross-Polytopes in the Euclidean 4-Space," Journal for Geometry and Graphics, vol. 4, no. 2, pp. 159–167, 2000.

[4] V. Muralidharan, N. Testard, C. Chevallereau, A. Abourachid, and P. Wenger, "Variable Stiffness and Antagonist Actuation for Cable-Driven Manipulators Inspired by the Bird Neck," Journal of Mechanisms and Robotics, vol. 15, June 2023.

[5] B. Fasquelle, P. Khanna, C. Chevallereau, D. Chablat, D. Creusot, S. Jolivet, P. Lemoine, and P. Wenger, "Identification and Control of a 3-X Cable-Driven Manipulator Inspired From the Bird's Neck," Journal of Mechanisms and Robotics, vol. 14, Feb. 2022. Publisher: American Society of Mechanical Engineers.

[6] A. van Riesen, M. Furet, C. Chevallereau, and P. Wenger, "Dynamic analysis and control of an antagonistically actuated tensegrity mechanism," in 22nd CISM IFToMM Symposium on Robot Design, Dynamics and Control (ROMANSY'2018), vol. 584 of ROMANSY 22 – Robot Design, Dynamics and Control Proceedings of the 22nd CISM IFToMM Symposium, June 25-28, 2018, Rennes, France, (Rennes, France), pp. 481–490, Springer, June 2018.

[7] B. Fasquelle, M. Furet, C. Chevallereau, and P. Wenger, "Dynamic modeling and control of a tensegrity manipulator mimicking a bird neck," in Advances in Mechanism and Machine ScienceProceedings of the 15th IFToMM World Congress on Mechanism and Machine Science, pp. 2087–2097, 2019.

[8] N. J. S. Testard, C. Chevallereau, and P. Wenger, "Comparison of Explicit and Implicit Numerical Integrations for a Tendon-Driven Robot," in Cable-Driven Parallel Robots (S. Caro, A. Pott, and T. Bruckmann, eds.), Mechanisms and Machine Science, (Cham), pp. 234–245, Springer Nature Switzerland, 2023.